Interstrand and AC-Loss Measurements on Rutherford-Type Cables for Accelerator Magnet Applications

R. Otmani, A. Devred, P. Tixador

***Abstract*—One of the main issues for particle accelerator magnets is the control of interstrand resistances. Too low resistances result in large coupling currents during ramping, which distort field quality, while too large resistances may prevent current redistribution among cable strands, resulting in degraded quench performance. In this paper, we review a series of interstrand resistance and AC-loss measurements performed on four Rutherford-type cables. The four cables have the same number of strands and similar outer dimensions, corresponding to LHC quadrupole cable specifications. The first cable is made from NbTi strands, coated with silver-tin alloy, the second one is made from bare Nb_3Sn strands, the third one is made also from bare Nb_3Sn strands but includes a 25-μm-thick stainless steel core between the strand layers, and the last one is made from Nb_3Sn strands plated with chromium. To cross-check the two measurement types and assess their consistency, we compare the coupling-current time constants determined from AC-loss measurements with estimates based on a simple analytical model and relying on measured interstrand resistances.**

***Index Terms*—Crossover and Adjacent Resistances, Interstrand Coupling Currents, Rutherford-Type Cables.**

I. Introduction

Accelerator magnet coils are wound from flat, two-layer, Rutherford-type cables, made up of a few tens of strands, twisted together. In such cables (see Fig. 1), the contacts at the crossovers between strands of the two layers and the contacts between adjacent strands of a same layer can engender low interstrand resistances. Low resistances favor current redistribution among cable strands, thereby increasing the stability against thermal perturbations [1]. However, when subjected to a time-varying magnetic field, the interstrand resistance network can be the seat of large coupling currents, which degrade field quality and quench performance [2], [3]. Hence, it is highly desirable to find a trade-off and to control interstrand resistances.

In a previous paper [4], we have described an experimental setup for *in-situ* interstrand resistance measurements and we discussed preliminary test results. In this paper, we described how the setup was also used for AC-loss measurements and we summarize a series of tests performed on four different cable samples. This work was carried out in the framework of a collaboration between Alstom/MSA and DAPNIA/STCM aimed at building a Nb_3Sn quadrupole magnet model [5], and its main goal was the determination of the best cable configuration.

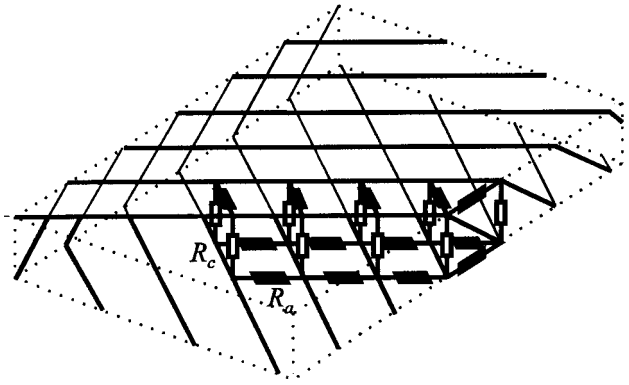

Fig. 1 Rutherford-type cable model.

II. Cable Samples

We measured four different cable samples: one NbTi cable provided by CERN, and three Nb_3Sn cables manufactured by Alstom/MSA. As summarized in Table I, the four cables have the same number of strands and similar outer dimensions. The CERN cable, referred to as LHC1, is an LHC quadrupole cable, made up of 0.825-mm diameter NbTi strands, coated with AgSn alloy [6]. The Alstom cables were developed as part of the collaboration with DAPNIA/STCM. Although the quadrupole magnet model will rely on 0.825-mm-diameter strands [7], cabling trials were carried out by Alstom/MSA using existing ITER-type strands with a 0.78-mm diameter [8]. These strands were produced according to the internal-tin process starting from billets of similar layouts. The first of the three cables, referred to as ALS1, uses plain strands with a copper-to-non-copper ratio of 1.2 to 1. The second cable, referred to as ALS2, uses the same strands as ALS1, but incorporates a 13-mm-wide, 25-μm-

Manuscript received September 17, 2000.
R. Otmani is with Alstom/MSA/Fils, 3bis avenue des 3 chênes, 90018 Belfort Cedex, France.
A. Devred is with CEA/Saclay, DSM/DAPNIA/STCM, 91191 Gif-sur-Yvette Cedex, France (arnaud.devred@cea.fr).
P. Tixador is with CRTBT/LEG, BP 166, 38042 Grenoble Cedex 9, France.
Web page: www-dapnia.cea.fr/Phys/Stcm/nb3sn

thick core, made up of annealed, 316L, stainless steel. As shown in

TABLE I
SALIENT CABLE PARAMETERS

	LHC1[a]	ALS1[b]	ALS2[b]	ALS3[b]
Strand Type	NbTi	Nb_3Sn	Nb_3Sn	Nb_3Sn
Strand Diameter (mm)	0.825	0.78	0.78	0.78
Strand Coating	AgSn	None	None	Cr
Strand Number	36	36	36	36
Cable Width (mm)	15.10	14.87	14.86	14.84
Mid-Thickness (mm)	1.480	1.410	1.427	1.412
Keystone Angle (°)	0.90	0.82	0.80	0.825
Pitch Length (mm)	100	73	73	84
Core	None	None	Yes	No

[a]Specifications [b]Manufacturer measurements

Fig. 2, the core is positioned between the two strand layers. The third cable, referred to as ALS3, uses chromium-plated strands with a copper-to-non-copper ratio of 1.4 to 1.

The NbTi cable was subjected to an annealing heat treatment at the end of cabling and was insulated with polyimide tapes. Upon reception at CEA/Saclay, it was cured, between two similar cable samples, at 185 °C during 30 minutes under 100 MPa, before being mounted in its sample holder (so as to simulate coil curing). The Nb_3Sn cables were not insulated and were mounted "as received" in their sample holders.

I. SAMPLE PREPARATION

The measurements were carried out in two phases, starting with interstrand resistances, followed by AC losses. They were performed on the same cable samples mounted in the same sample holders, with no direct intervention on the cable pieces being characterized.

In preparation for interstrand resistance measurements, and as illustrated in Fig. 3, the cables were placed in 100-mm-long stainless steel (316L) sample holders, made up of a U-shaped base covered by a T-shaped top. The top was tied up to the bottom by means of two rows of four screws (one on each side), designed to apply a known pressure to the cable broad face. The cable samples were neatly cut at one end and were untwisted at the other. Six of the untwisted strands were soldered to current leads while up to 15 strands were equipped with voltage taps. The sample and their holders were mounted (each at a time) on an insert, that was shoved into the bore of a superconducting dipole magnet and cooled down to 4.2 K.

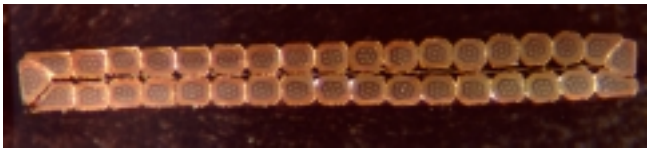

Fig. 2. Nb_3Sn Rutherford-type cable with a 25-µm-thick stainless steel core.

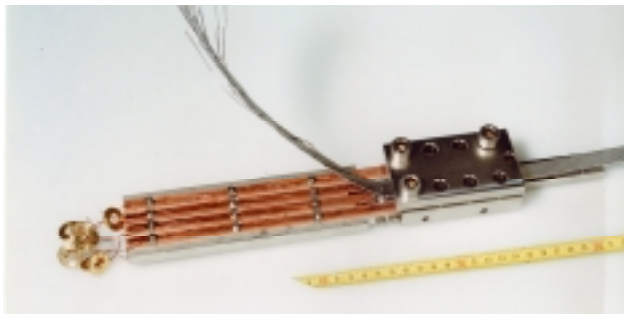

Fig. 3. Sample preparation for interstrand resistance measurements.

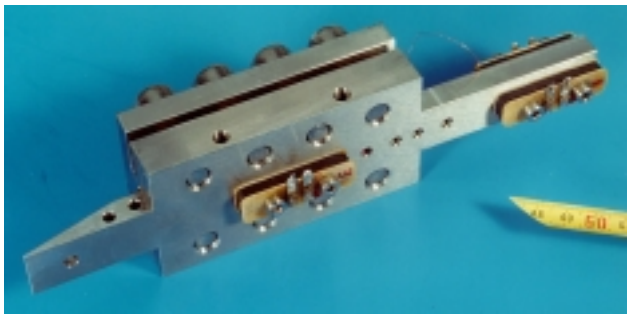

Fig. 4. Sample preparation for ac-loss measurements.

Prior to instrumentation and mounting on the insert, all Nb_3Sn samples were subjected, in their sample holders, to the heat-treatment required for Nb_3Sn compound formation. ALS1 was heat-treated at CEA/Saclay in a flow of argon gas, while ALS2 and ALS3 were heat-treated at Alstom/MSA in vacuum. The heat treatment parameters were the same at both places: ramp at 6 °C per hour up to 660 °C followed by a 240-hour plateau at 660 °C. The tops of the sample holders were put in place prior to heat treatment and were never removed. After heat treatment, it was determined that the ALS1 screws were tightened to torques corresponding to about 20 MPa on the cable, while those of ALS2 and ALS3 were found to be more or less loose.

Once the interstrand measurements were completed, the insert was taken out for preparation of AC-loss measurements. All untwisted strands were cut at the sample extremity, leaving only the untouched cable piece pressed in the sample holder. Also, and as illustrated in Fig. 4, three identical pick-up coils were mounted on the sample holder: one *main* coil, positioned right above the cable sample, to embrace all the field effects it produces, and two *reference* coils positioned at some distance from the sample, to be insensitive to cable magnetization. The coils were 41-mm long, 10-mm wide and were made up of 150 turns. Then, the assembly was re-inserted into the dipole magnet and cooled down again at 4.2 K.

II. INTERSTRAND RESISTANCE MEASUREMENTS

The test procedure has been described in detail elsewhere [4]. After tightening of the sample-holder screws to the desired torque, insertion into the vertical dewar, and

cooldown to 4.2 K, the background dipole magnet was ramped up to a given and constant field (typically 0.4 T). The measurements themselves consisted of selecting a pair of current leads, supplying a small current (typically between 0 and 250 A), and measuring the voltages between the instrumented strands and the negative current lead. They were repeated for all available pairs of current leads.

The measured data were analyzed so as to estimate effective values of *crossover* and *adjacent* resistances. In the model of Fig. 1, the strands are represented by equipotential lines. Over a twist pitch, each strand crosses two times every other strand. The crossings are represented by elementary resistances, referred to as *crossover resistances*, R_c. The points where the crossover resistances are connected to the lines define the network nodes. Furthermore, the continuous contacts between adjacent strands are represented by discrete elementary resistances, referred to as *adjacent resistances*, R_a, connected to the network nodes. Over a pitch length of a N-strand cable, each strand encounters ($2N$–2) crossover resistances and is connected to each of its neighbors by ($2N$) adjacent resistances.

Starting from this circuit, and assuming that R_a and R_c are uniform, we developed a computer model representing a cable pitch length. The code inputs are: number of cable strands, initial values of R_c and R_a, numbers of the strands connected to current leads, and supplied current value. The main code routine computes the potentials at the network nodes, including those at the cable end where the voltage taps are located. Next, the code carries out an optimization and iteratively determines the values of R_c and R_a minimizing the root mean square of the difference between computed potentials and measured voltages.

Table II summarizes the optimization results, along with estimates of the residual errors, for the various cable samples at 100 MPa and 0.4 T. The crossover resistance measured on LHC1 is consistent with what can be expected for such a cable and meets LHC specifications [9]. The R_c-value obtained on ALS1 is very low, and may cause sizeable crossover coupling currents. The R_c- and R_a-values obtained on ALS3 are very high, and may prevent current redistribution among cable strands. ALS2 seems to offer a good compromise, with high R_c-values and low R_a-values, but this interstrand configuration is almost opposite to that of LHC1 and has, so far, never been tried on a real magnet. This configuration is, nevertheless, the one we have chosen for our quadrupole magnet model. Note that the interstrand resistances measured on ALS1 and ALS2 are consistent with resistance values derived from calorimetric measurements on similar cables [4], [10].

TABLE II
INTERSTRAND RESISTANCES AT 100 MPA

	LHC1	ALS1	ALS2	ALS3[a]
R_c (μΩ)	21	1.1	275	505
R_a (μΩ)	168	10.3	1.7	151
Residual Error (%)	6.9	9.5	12	

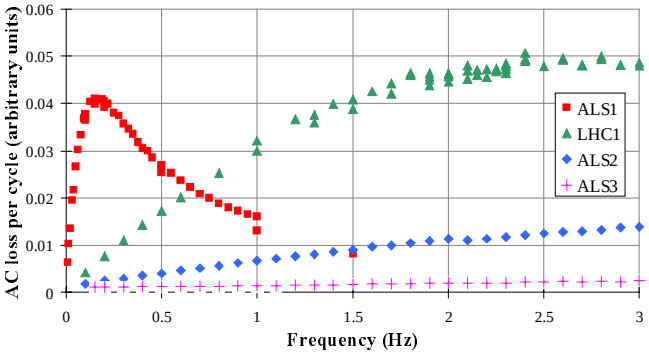

Fig. 5. Summary plot of energy loss per cycle as a function of frequency.

[a]Wide data dispersion

III. AC LOSS MEASUREMENTS

The test procedure for AC-loss measurements was as follows. After cutting the untwisted strands and mounting the pick-up coils, the sample-holder screws were tightened again to torque values corresponding to 100 MPa on the cable, and the insert was repositioned in the dewar. The dipole magnet was ramped up to a base field of 0.3 T (to limit hysteresis losses), to which we superimposed a sinusoidal oscillation with a frequency between 0 and 3 Hz and an amplitude between 0.05 and 0.2 T. One of the reference pick-up coils was used to measure the background field, while the other was subtracted from the main coil, to buck out the background field and provide a signal directly proportional to cable magnetization. The signal issued from the reference coil and the bucked signal were integrated (using analog integrators) and recorded into the buffer memory of a chart recorder, before being transferred to a PC. The AC-loss per cycle was determined by computing numerically the product of the two signals and by integrating it over one period.

Unfortunately, the system has not been calibrated and the data can only be used for inter-cable comparisons. The values of AC-loss per cycle quoted in this paper are normalized to the square of the amplitude of the sinusoidal field variations and are given in arbitrary units.

It is worth mentioning that we performed two additional series of measurements: one on an empty sample holder, and another one where we replaced the cable by a stack of 10 samples cut in the stainless steel core used in ASL2. In both cases, the recorded signals were lost in the noise, meaning that the contributions from the sample holder and from the stainless steel core are negligible.

Figure 5 presents a summary plot of measured AC loss per cycle as a function of frequency for the various cable samples at 100 MPa. As expected, the cables exhibiting the most losses are the Nb_3Sn cable with bare strands (ALS1), followed by the NbTi cable with AgSn-coated strands (LHC1). The curve for the Nb_3Sn cable with a stainless steel core (ALS2) shows a slow and quasi-linear increase, which, in comparison to the ALS1 curve, confirms the drastic loss reduction brought about by the core. The effect is even more pronounced for the Nb_3Sn cable with chromium plated

strands (ALS3) whose curve is almost flat.

IV. Time Constants

"AC-loss vs. Frequency" curves can usually be fitted by a function of the form [8]

$$W = W_0 \frac{2\pi f\tau}{1+4\pi^2 f^2\tau^2} \qquad (1)$$

where W is the measured AC-loss per cycle at frequency f, W_0 is a constant coefficient, and τ is the so-called *time constant* of the interstrand coupling currents. The time constants, τ_{mes}, determined using the above fit are summarized in Table III.

The τ_{mes}-values can be compared to theoretical ones derived from either an analytical model or a computer simulation. In the analytical model, the time constants, τ_c and τ_a, associated with the crossover and adjacent coupling currents, are estimated from

$$n\tau_c \approx \frac{\mu_0 N^2 wL}{120hR_c} \qquad (2a) \quad \text{and} \quad n\tau_a \approx \frac{\mu_0 wL}{6hR_a} \qquad (2b)$$

Here, μ_0 is the permeability of vacuum ($4\pi 10^{-7}$ H/m), N is the number of strands, w is the cable width, h is the cable mid-thickness, L is the pitch length, and n is a shape factor, which, for a single cable, can be taken as [11]

$$n \approx \frac{\pi}{2} \frac{1}{\arctan\frac{2h}{w}} \qquad (3)$$

Thereafter, let τ_{theo} designate the maximum of τ_c and τ_a.

Furthermore, the above expression of τ_c can be compared to the one given in Ref. [12], referred to as $\tau_{verweij}$

$$\tau_{verweij} \approx C \frac{(N^2-4N)L}{R_c} \qquad (4)$$

where C is a constant, determined from a computer model, and which, for our cables, is of the order of $1.7\ 10^{-8}$.

The computed values of τ_{theo} and $\tau_{verweij}$ are summarized in Table III. They are in fair agreement with the measured ones, thereby demonstrating the consistency of the interstrand resistance and AC-loss measurements. It appears also that the estimates provided by the analytical formulae are reasonable.

TABLE III
Time Constants at 100 mA

	LHC1	ALS1	ALS2	ALS3
τ_{mes} (ms)	96	1015	18	1.6
Shape Factor	8.11	8.38	8.28	8.35
Dominating Resistance	R_c	R_c	R_a	R_c
τ_{theo} (ms)	81	1133	11	2.8
$\tau_{verweij}$ (ms)	93	1300	n/a	3.3

It is worth mentioning that the time constants of the intrastrand coupling currents have been measured independently on the Nb_3Sn strands and are: 0.31 ms for the strand used in ALS1 and ALS2, and 0.19 ms for the strand used in ALS3. These values are well below those given in Table III, which confirms the domination of the interstand coupling currents. The domination may be less clear for the NbTi strand, where the time constant of the intrastrand coupling currents can reach 20 ms [12], but no independent measurements were carried out.

V. Conclusion

We performed two types of measurements to assess the behavior of different Rutherford-type cable configurations under time-varying fields. The two measurement types yield consistent results, and, among the Nb_3Sn cables, lead us to favor the one with bare strands and a stainless steel core. This cable is now under production at Alstom/MSA and will be used to wind a short quadrupole magnet model.

Acknowledgments

The authors wish to thank the technical staff of DAPNIA/STCM, and more particularly C. Génin. They also wish to thank L. Bacquart, G. Curnier, C. Mangeant, S. Sanchez, and T. Schild for their valuable contributions.

References

[1] M.N. Wilson and R. Wolf, "Calculation of minimum quench energies in Rutherford-type cables," *IEEE Trans. Appl. Supercond.*, Vol. 7 No. 2, pp. 950–953, 1997

[2] A. Devred and T. Ogitsu, "Ramp-rate sensitivity of SSC dipole magnet prototypes," *Frontiers of Accelerator Technology*, World Scientific, Singapore, pp. 184–308, 1996.

[3] T. Ogitsu, A. Devred, and V. Kovachev, "Influence of inter-strand coupling current on field quality of superconducting accelerator magnets," *Particle Accelerators*, Vol. 57, pp. 215–235, 1997.

[4] A. Devred, L. Bacquart, et al., "Interstrand resistance measurements on Nb_3Sn Rutherford-type cables," *IEEE Trans. Appl. Supercond.*, Vol. 9 No. 2, pp. 722–726, 1999.

[5] A. Devred, M. Durante, et al., "Development of a Nb_3Sn quadrupole magnet model," in these Proceedings.

[6] "Technical specification of the dipole outer layer and quadrupole superconducting cable for the LHC," Internal Note LHC–MMS/97–153, CERN, Geneva, Switzerland, July 1997.

[7] M. Durante, P. Bredy, et al., "Development of a Nb_3Sn multifilamentary wire for accelerator magnet applications," Presented at ICMC2000, Rio de Janeiro, Barzil, June 2000.

[8] R. Otmani, "Etudes de cables Nb_3Sn pour quadripôles supraconducteurs," PhD dissertation (in French), Internal Report DAPNIA/STCM 99–1001, CEA/Saclay, Gif sur Yvette, France, 26 Octobre 1999.

[9] D. Richter, J.D. Adam, *et al.*, "DC measurements of electrical contacts between strands in superconducting cables for the LHC magnets," *IEEE Trans. Appl. Supercond.*, Vol. 7 No. 2, pp. 786–792, 1997.

[10] M.D. Sumption, E.W. Collings, *et al.*, "AC Loss and contact resistance in Nb_3Sn Rutherford cables with and without a stainless steel core," *Adv. Cryo. Eng. (Materials)*, Vol. 44(B), pp. 1077–1084, 1998.

[11] P. Tixador and D. Leroy, "Coupling losses in superconducting cables: models and measurements," Internal Note CERN–SPS/89, CERN, Geneva, Switzerland, 27 January 1989.

[12] A.P. Verweij, “Electrodynamics of superconducting cables in accelerator magnets,” Ph.D Dissertation, Twente University, Enschede, the Netherlands, p. 78, 15 September 1995.